Mesoscopic *p*-wave superconductor near the phase transition temperature

Bor-Luen Huang and S.-K. Yip

Institute of Physics, Academia Sinica, Taipei, Taiwan

We study the finite-size and boundary effects on a *p*-wave superconductor in a mesoscopic rectangular sample using Ginzburg-Landau and quasiclassical Green's function theory. Apart from a few very special cases, we find that the ground state near the critical temperature always prefers a time-reversal symmetric state, where the order parameter can be represented by a real vector. For large aspect ratio, this vector is parallel to the long side of the rectangle. Within a critical aspect ratio, it has instead a vortexlike structure, vanishing at the sample center.

Studies of multicomponent superfluids and superconductors have excited many for decades because of the diversity of textures, complex vortex structures, and collective modes. The superfluid ^{3}He with a spin-triplet order parameter[1,2] is a well-established example. Many studies also show that superconductors with multicomponent order parameters can also be found in, for example, UPt$_3$[3,4] and Sr$_2$RuO$_4$.[5,6] Recently, studies of a multicomponent superconductor in a confined geometry draw much attention due to advancements in nanofabrication. Experiments claimed to find half-quantum vortices[7] and the Little-Parks effect[8] in the Sr$_2$RuO$_4$ quantum ring. Surfaces are expected to have nontrivial effects on such superconductors. Some theoretical works show that surface currents are present in broken time-reversal symmetric superconductors.[9–11] In considering Ru inclusions, Sigrist and his collaborators[12] have shown that a time-reversal symmetry state can be favored near the interface between Ru and Sr$_2$RuO$_4$ due to the boundary conditions. In our previous work,[13] considering a thin circular disk with smooth boundaries and applying the Ginzburg-Landau (GL) theory, we have shown that a two-component *p*-wave superconductor can exhibit multiple phase transitions in a confined geometry. At zero magnetic field, the superconducting transition from the normal state was found to be always first to a time-reversal symmetric state (with an exception which occurs only far away from the isotropic weak-coupling limit), even though the bulk free energy may favor a broken time-reversal symmetry state, which can exist at a lower temperature. This time-reversal symmetric state has a vortexlike structure, with the order parameter vanishing at the center of the disk. We have also argued there that these features are general, do not rely on the GL approximation, and should also exist for general geometries.[14]

In this paper, we investigate this question further by considering rectangular and square samples, employing both the GL and the quasiclassical (QC) Green's function methods. Within GL, for rectangular samples with large aspect ratios, we show that the phase transition from the normal to the superconducting state is second order and is to a state with the order parameter being a real vector parallel to the long side of the sample. For smaller aspect ratios, the state near the transition temperature is again a time-reversal symmetric state with a vortex at the center, except for a square and only for gradient coefficients far away from the weak-coupling limit, much like what we found for the circular disk. At not too

small sizes, the results from QC are qualitatively similar to GL except for the critical sizes and aspect ratios obtained. At very small sizes, however, the QC calculation suggests that a more complicated situation can arise for some special aspect ratios. The transition can either become first order, or perhaps into a state with a more complicated order parameter. In this paper, we shall mostly concentrate on the parameter region where the phase transition is second order and leave the detailed investigation of the above-mentioned special case to the future.

We shall thus consider a superconductor where its orbital part is given by $\vec{\eta} = \eta_x \hat{x} + \eta_y \hat{y}$. We shall consider the dependencies of η_x and η_y on the coordinates x, y, assuming that they are constant along the z direction. We assume the length of the sample in the x direction is L and the width in the y direction is W, and these surfaces are smooth. The effects of a rough boundary have been discussed in Ref. 13 for the circular disk. We shall also limit ourselves to zero external magnetic fields. Near the second-order transition temperature, the magnetic field generated by the supercurrent is also negligible, hence the vector potential can always be ignored.

First, we study this system via the GL theory. The GL free energy density per unit area for the bulk, $\mathcal{F}_b$, can be written as

$$\mathcal{F}_b = \alpha(\vec{\eta}^* \cdot \vec{\eta}) + \dots, \tag{1}$$

where $\alpha = \alpha'(t - 1)$ with $\alpha' > 0$, $t \equiv T/T_c^0$ is the ratio of the temperature T relative to the bulk transition temperature T_c^0, and ... represents terms higher power in the order parameter which are irrelevant below since we are interested only in the physics at the (modified) transition temperature T_c. In the presence of spatial variations, there is an additional contribution to the free energy given by

$$\mathcal{F}_g = K_1(\partial_j \eta_l)(\partial_j \eta_l)^* + K_2(\partial_j \eta_j)(\partial_l \eta_l)^*$$
$$+ K_3(\partial_j \eta_l)(\partial_l \eta_j)^* + K_4[(\partial_x \eta_x)^2 + (\partial_y \eta_y)^2], \tag{2}$$

where repeated indices j, l in the first three terms are summed over x, y, and the last term describes crystal anisotropy.[15] Within a weak-coupling approximation, particle-hole symmetry, and for an isotropic Fermi surface, $K_1 = K_2 = K_3 > 0$ and $K_4 = 0$, but we shall treat these coefficients as general parameters.

The GL equations need to be accompanied by boundary conditions. The perpendicular component of the order parameter at the surface should vanish.[17] Thus, for a point at

the surface where the normal is $\hat{n}$, $\hat{n} \cdot \vec{\eta} = 0$. For a smooth surface, the parallel component $\eta_\parallel$ should have a vanishing normal gradient,[17] that is, at the surface, $(\hat{n} \cdot \nabla)\eta_\parallel = 0$.

GL equations for $\eta_{x,y}$ can be obtained by the variation principle. Near the critical temperature, we can linearize these equations. The easiest way to match the boundary conditions is to superimpose the Fourier components. Written in matrix form, the GL equations for the Fourier component $\vec{q}$ become

$$\begin{pmatrix} K_1 q^2 + K_{234} q_x^2 & K_{23} q_x q_y \\ K_{23} q_x q_y & K_1 q^2 + K_{234} q_y^2 \end{pmatrix} \begin{pmatrix} \eta_{x,\vec{q}} \\ \eta_{y,\vec{q}} \end{pmatrix}$$
$$= \alpha'(1-t) \begin{pmatrix} \eta_{x,\vec{q}} \\ \eta_{y,\vec{q}} \end{pmatrix}. \tag{3}$$

Here, $\vec{q}$ is the wave vector, $q^2 = q_x^2 + q_y^2$, $K_{23} = K_2 + K_3$, and $K_{234} = K_2 + K_3 + K_4$.

It is easy to find that, if $q_x = 0$ or $q_y = 0$, Eq. (3) decouples. We obtain either (i) $\eta_{x,\vec{q}} \neq 0$ with $\eta_{y,\vec{q}} = 0$ or (ii) $\eta_{y,\vec{q}} \neq 0$ with $\eta_{x,\vec{q}} = 0$. We call these solutions A phases. In case (i), we have two possibilities. One is $\hat{q} = \hat{x}$ and the critical temperature is determined by $\alpha'(1-t) = K_{1234} q^2$. Because $\eta_x(x)$ is independent of y, the possible solutions are $\eta_x = X \sin \frac{m\pi x}{L}$, satisfying the boundary conditions, $\eta_x = 0$, at $x = 0$ and L. Here X is a constant and m is an integer. The best choice is $m = 1$ and the critical temperature is $\alpha'(1-t) = K_{1234}(\pi/L)^2$. We call this the A_1 phase. The other is $\hat{q} = \hat{y}$. The order parameter $\eta_x(y)$ is independent of x. Thus it is not possible to satisfy the boundary conditions at $x = 0$ and L. In case (ii), the best solution is $\eta_y \propto \sin \frac{\pi y}{W}$, which is just the solution in case (i) with $x \leftrightarrow y$. The critical temperature is determined by $\alpha'(1-t) = K_{1234}(\pi/W)^2$. We call this the A_2 phase.

If both q_x and q_y are nonzero, both $\eta_{x,\vec{q}}$, $\eta_{y,\vec{q}}$ are finite. We define this kind of solution as the B phase. To simplify the calculations, we ignore crystal anisotropy for the moment, and set $K_4 = 0$. From Eq. (3), we find the smallest eigenvalue is $K_1 q^2$ (for $K_{23} > 0$). To have the normal component to the surfaces at $x = 0$ and L to vanish, η_x must have the factor $\sin(m\pi x/L)$, where m is an integer. Because the boundary conditions $\partial \eta_x / \partial y = 0$ at $y = 0$ and W, η_x should be proportional to $\cos(n\pi y/W)$, with n also an integer. We can use the same arguments for η_y. Therefore

$$\eta_x = X \sin \frac{m\pi x}{L} \cos \frac{n\pi y}{W},$$
$$\eta_y = Y \cos \frac{m\pi x}{L} \sin \frac{n\pi y}{W}. \tag{4}$$

The critical temperature is highest for $m = n = 1$, and thus determined by $\alpha'(1-t) = K_1[(\pi/L)^2 + (\pi/W)^2]$. In order to satisfy Eq. (3), we need $(\pi/L)X + (\pi/W)Y = 0$, which means X and Y are relatively real and have opposite signs.

Comparing the transition temperatures of the A and B phases, we find that the system prefers the A_1 phase for $L \gg W$. For $L \sim W$, it prefers the B phase. We define the aspect ratio of the sample as $\rho = L/W$. The critical aspect ratio separating these two phases is

$$\rho_c = \sqrt{K_{23}/K_1}. \tag{5}$$

With the same reasoning, the system is in the A_2 phase for $W \gg L$ but prefers the B phase if ρ is larger than
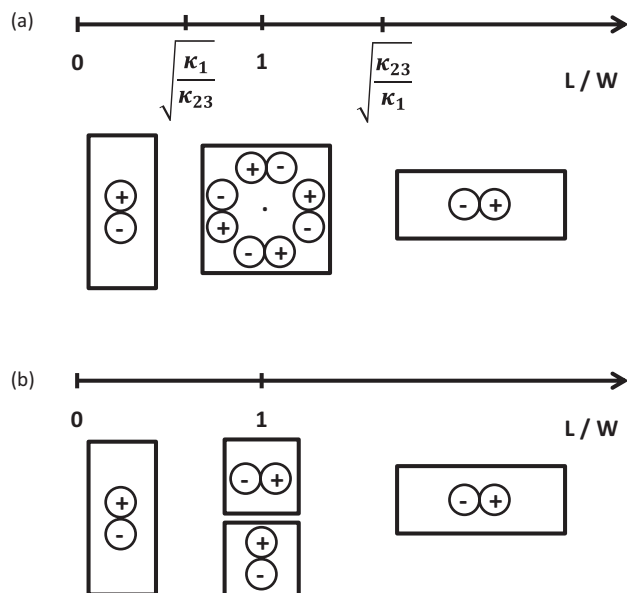

FIG. 1. GL phase diagram at the transition temperature. $K_4 = 0$. (a) $K_{23}/K_1 > 1$; (b) $K_{23}/K_1 < 1$.

$\rho_c^{-1} = \sqrt{K_1/K_{23}}$. The phase diagram is shown in Fig. 1(a). The cartoon pictures under the ruler are used to specify the main characteristic of the order parameter in the corresponding phases. The solution for the middle case (B phase) is qualitatively the same as the circular disk in Ref. 13. Because of the relatively real coefficients in Eq. (4), we can represent $\vec{\eta}$ by a real vector, as done in the inset of Fig. 2(c). It is clear that the order parameter forms a vortexlike structure, and vanishes at the sample center.

When crystal anisotropy is included, the critical ratio becomes

$$\rho_c = \sqrt{\frac{K_{1234} K_{234} - K_4(K_{23} + K_{234})}{K_1 K_{1234}}}. \tag{6}$$

It reduces to Eq. (5) for $K_4 = 0$. For small K_4, the critical ratio is $\sqrt{2 - K_4/K_{123}}$ within the weak-coupling limit. It shows that the crystal anisotropy for $K_4 > (<)0$ stabilizes (destabilizes) the order parameter with the direction parallel to the long side of the sample. The phase diagram is similar to Fig. 1(a) except a smaller (larger) region for the vortex state. We ignore crystal isotropy in the following.

With decreasing K_{23}/K_1, the stability region for the B phase becomes narrower. This phase diagram [Fig. 1(a)] will change qualitatively if $K_1 > K_{23}$ The B phase is never stable (at T_c), and the system is in the A_1 phase if $\rho > 1$, and in the A_2 phase if $\rho < 1$. The square sample $\rho = 1$ forms a special case, where the system still has C_4 symmetry in real space, and the A_1 and A_2 phases are therefore degenerate. One can combine these two solutions with a phase difference. As a result, if the higher order terms in Eq. (1) for the bulk free energy prefer a time-reversal-symmetry-broken state, then the system would enter such a state directly at T_c. Therefore, the phase diagram becomes Fig. 1(b) for $K_{23} < K_1$, where the ground state at $\rho = 1$ should break the time-reversal symmetry.[18]

Our results for the square here provide further understanding of those we obtained earlier for the circular disk.[13] There, we found that, for $K_{1,2,3}$ near the weak-coupling values ($K_1 = K_2 = K_3$) the phase transition from the normal state is always to the state (named $n = 1$ there) which preserves time reversal but with a vortex at the center. That phase obviously has the same qualitative behavior as our *B* phase here. For sufficiently small K_{23}/K_1, we found that the system can enter a broken time-reversal symmetry state directly. We find the same results here though the critical value for K_{23}/K_1 obviously can depend on the geometry.

In order to check the validity of the phase diagram from the GL theory, we employ the quasiclassical (QC) Green's function theory. For simplification, we focus on the isotropic and weak-coupling case. As shown in Ref. 13, we have, after linearizing in the order parameter,

$$(2i\epsilon_n + iv_f\hat{p}\cdot\vec{\nabla})f = 2i\pi(\text{sgn}\epsilon_n)\Delta, \qquad (7)$$

where $f(\hat{p},\epsilon_n,\vec{r})$ and $\Delta(\hat{p},\vec{r})$ describe separately the off-diagonal parts of the QC propagator and pairing function, $\hat{p}$ is the momentum direction, ϵ_n is Matsubara frequency, and v_f is the Fermi velocity. With the pairing interaction written as $V_1\hat{p}\cdot\hat{p}'$, the gap equation reads

$$\Delta(\hat{p},\vec{r}) = N(0)TV_1\sum_n\langle(\hat{p}\cdot\hat{p}')f(\hat{p}',\vec{r},\epsilon_n)\rangle, \qquad (8)$$

where the angular bracket denotes angular average over $\hat{p}'$ and $N(0)$ is the density of states at the Fermi level. For our square geometry and assuming smooth surfaces, we have the boundary conditions $f(\theta) = f(\pi - \theta)$ at $x = 0$ and L and $f(\theta) = f(-\theta)$ at $y = 0$ and W. Here θ is the angle between $\hat{p}$ and $\hat{x}$.

Before solving the case in a confined rectangle, we like to mention the connection between the GL theory and the QC theory for the bulk. To zeroth order in gradient, one finds

$$1 = \pi N(0)V_1T_c^0\sum_{\epsilon_n}\frac{1}{2|\epsilon_n|}, \qquad (9)$$

which defines the bulk transition temperature T_c^0. The first order for f is odd in ϵ_n and will not contribute to the gap equation. In the second order, we recover the GL theory with

$$\frac{K_1}{\alpha'} = 2\pi T_c^0\sum_{\epsilon_n}\frac{v_f^2}{4|\epsilon_n|^3}\langle\cos^2\theta\sin^2\theta\rangle, \qquad (10)$$

and similar expressions for $K_{2,3}$, with $K_1 = K_2 = K_3$. Our equations are consistent with those in Refs. 1,2 and 16.

For the A_1 phase, we shall show that we can have a self-consistent solution in the QC theory with

$$\Delta(\hat{p},\vec{r}) = X\sin\frac{\pi x}{L}\cos\theta, \qquad (11)$$

the order parameter suggested by the GL theory. One finds that f is independent of y. With the ansatz,

$$f(\theta,\epsilon_n;x) = C_1(\theta,\epsilon_n)\sin\frac{\pi x}{L} + C_2(\theta,\epsilon_n)\cos\frac{\pi x}{L}, \qquad (12)$$

satisfying the boundary conditions, solving for $C_{1,2}(\theta,\epsilon_n)$ via Eq. (7) and using (9), we find

$$\ln\frac{T_c^0}{T_c} = 2\pi T_c\sum_{\epsilon_n=-\infty}^{\infty}\left\langle\frac{\left(\frac{v_f\pi}{L}\right)^2\cos^4\theta}{4|\epsilon_n|^3\left[1 + \frac{(\frac{v_f\pi}{L}\cos\theta)^2}{4\epsilon_n^2}\right]}\right\rangle. \qquad (13)$$

For large L, one can replace the bracket in the denominator by 1, and the left-hand side by $(1 - t)$, recovering the GL result using Eq. (10). Hence we see that, beyond GL, one needs simply to include extra factors in the denominator of Eq. (13) and include the ln on the left-hand side.

Now, we consider the *B* phase. The order parameter is

$$\Delta(\hat{p},\vec{r}) = X\sin\frac{\pi x}{L}\cos\frac{\pi y}{W}\cos\theta + Y\cos\frac{\pi x}{L}\sin\frac{\pi y}{W}\sin\theta. \qquad (14)$$

From previous experience, it suggests that the solution has the following form:

$$f = C_1(\theta,\epsilon_n)\sin\frac{\pi x}{L}\cos\frac{\pi y}{W} + C_2(\theta,\epsilon_n)\cos\frac{\pi x}{L}\sin\frac{\pi y}{W}$$
$$+ C_3(\theta,\epsilon_n)\cos\frac{\pi x}{L}\cos\frac{\pi y}{W} + C_4(\theta,\epsilon_n)\sin\frac{\pi x}{L}\sin\frac{\pi y}{W}. \qquad (15)$$

To simplify writing, let $A = \pi v_f/L$, $B = \pi v_f/W$. Again solving for f from (7), we obtain the following coupled linear equations in X,Y:

$$X\ln\frac{T_c^0}{T_c} = 2\pi T_c\sum_{\epsilon_n}\left\langle\frac{[(c_1 + c_2)\cos^2\theta]X + c_3Y}{|\epsilon_n|D}\right\rangle. \qquad (16)$$

$$Y\ln\frac{T_c^0}{T_c} = 2\pi T_c\sum_{\epsilon_n}\left\langle\frac{[(c_1 + c_2)\sin^2\theta]Y + c_3X}{|\epsilon_n|D}\right\rangle. \qquad (17)$$

Here $c_1 = (A^2\cos^2\theta + B^2\sin^2\theta)/(4\epsilon_n^2)$, $c_2 = (A^2\cos^2\theta - B^2\sin^2\theta)^2/(4\epsilon_n^2)^2$, $c_3 = (AB\sin^2\theta\cos^2\theta)/(2\epsilon_n^2)$, and $D = 1 + 2c_1 + c_2$. The critical temperature of the *B* phase is determined by the point which allows nontrivial X and Y. We note that if one keeps only the lowest orders in A^2 and B^2, $D \to 1$, and replaces the ln's on the left-hand side by $(1 - t)$, then Eqs. (16) and (17) recover the corresponding equations (3) in the GL theory.

In Fig. 2(a), we compare the critical temperatures for different sizes of square samples between the GL and QC theories. We use the coherence length $\xi \equiv \sqrt{K_{123}/\alpha'}$ as the unit for length ($\xi = 0.199909v_f/T_c^0$ for QC). In the GL theory, $(1 - t)$, the relative suppression of critical temperature, is inversely proportional to the square of the length scale of the system. Therefore it is more convenient to set the vertical axes of the phase diagram to be $(\xi/L)^2$. We obtain the straight line with crosses for the critical temperature of the *A* phase and the line with pluses for that of the *B* phase. It shows that the system prefers the *B* phase. On the other hand, we also present the critical temperatures calculated from the QC theory. The line with squares is for the *B* phase and the line with circles is for the *A* phase. As expected, it shows that the results from the QC theory are consistent with those from the
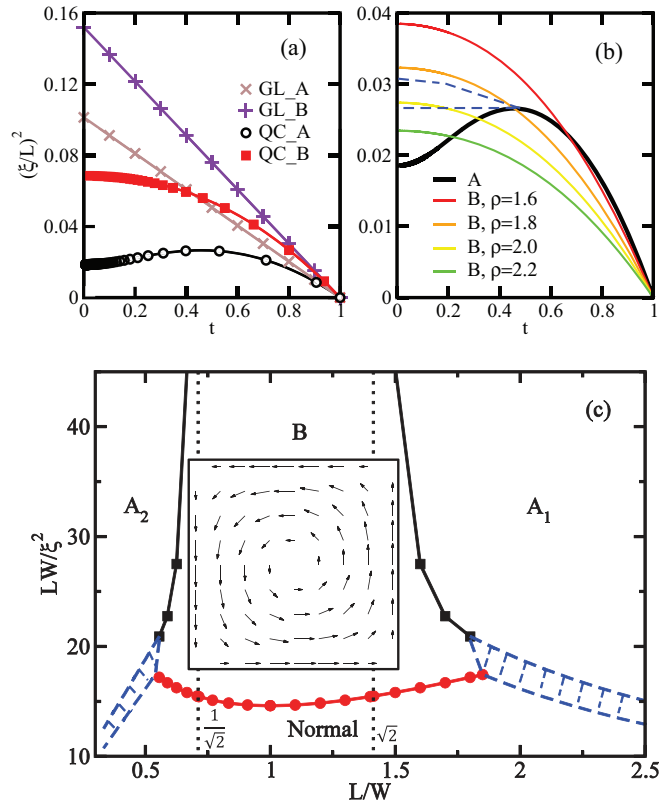
FIG. 2. (Color online) (a) Critical temperatures from GL and QC theories for square samples. (b) Critical temperatures in QC theory for different ρ's. As the size of the system is reduced, the ground state near the critical temperature can change from A to B. The possible first-order phase transition is indicated in the region between dash lines. (c) Phase diagram for different sizes. The white regions correspond to second-order normal to superconducting transitions; the dashed regions indicate possible first-order phase transitions. (Inset) Order parameter for a square sample. Note that all results are for $K_1 = K_2 = K_3$. ξ is the coherence length.

GL theory near $t = 1$, corresponding to $\xi/L \ll 1$. In addition to the fact that the B phase is still preferred, we see that the

critical temperature is more suppressed than GL as the size of the system is smaller.[19]

As the aspect ratio ρ becomes larger than 1, the GL theory shows that there is a phase transition from the B phase to the A phase as ρ increases beyond the critical ratio $\sqrt{K_{23}/K_1}$ [Fig. 1(a)]. In Fig. 2(b), we find that this critical ratio ($\sqrt{2}$ here) still applies for large systems. However, we find that the B phase occupies a slightly larger ρ region when the size decreases. An example is in Fig. 2(b), where we show that the system processes a phase transition from the A phase (thick black line) to the B phase for $\rho = 1.6$ (thin red line) around $t = 0.67$ as the size of the system becomes smaller. As the aspect ratio increases further, the situation becomes more complicated because the phase boundary for the A phase is not a monotonic function in t. The shape of the curve suggests that, at lower temperatures, the transition from the normal to the superconducting state cannot be a second-order transition to the A_1 phase as described here. One possibility is a first-order phase transition between the normal and the superconducting A_1 phase, analogous to Ref. 20. However, transition into a more exotic order parameter structure cannot be ruled out.[21] We shall leave the detailed investigation of this question for the future. For illustrative purposes, we indicate the resulting phase diagram by postulating a first-order transition line somewhere between the two dashed lines in Fig. 2(b). Our obtained phase diagram for the normal to superconducting transition, with instead now the sample area as the vertical axis, is as shown in Fig. 2(c). For the square samples, the stable superconducting phase is the B phase, with a vortexlike structure at the center, similar to the $n = 1$ state in Ref. 13 obtained in the disk geometry.

In conclusion, we studied a two-component p-wave superconductor in a rectangular geometry near its transition temperature. The order parameter can behave differently depending on the aspect ratio and size. Except for some special regions in parameter space, the phase always preserves time-reversal symmetry. Our results give further support to those obtained in Ref. 13.

[1]A. J. Leggett, Rev. Mod. Phys. **47**, 331 (1975).

[2]D. Vollhardt and P. Wölfle, *The Superfluid Phases of Helium 3* (Taylor and Francis, London, 1990).

[3]J. A. Sauls, Adv. Phys. **43**, 113 (1994).

[4]Robert Joynt and Louis Taillefer, Rev. Mod. Phys. **74**, 235 (2002).

[5]A. P. MacKenzie and Y. Maeno, Rev. Mod. Phys. **75**, 657 (2003).

[6]Y. Maeno, S. Kittaka, T. Nomura, S. Yonezawa, and K. Ishida, J. Phys. Soc. Jpn. **81**, 011009 (2012).

[7]J. Jang *et al.*, Science **331**, 186 (2011).

[8]X. Cai, Y. A. Ying, N. E. Staley, Y. Xin, D. Fobes, T. Liu, Z. Q. Mao, and Y. Liu, arXiv:1202.3146.

[9]M. Matsumoto and M. Sigrist, J. Phys. Soc. Jpn. **68**, 994 (1999); **68**, 3120(E) (1999).

[10]M. Stone and R. Roy, Phys. Rev. B **69**, 184511 (2004).

[11]J. A. Sauls, Phys. Rev. B **84**, 214509 (2011).

[12]M. Sigrist and H. Monien, J. Phys. Soc. Jpn. **70**, 2409 (2001); H. Kaneyasu, N. Hayashi, B. Gut, K. Makoshi, and M. Sigrist, *ibid.* **79**, 104705 (2010).

[13]Bor-Luen Huang and S.-K. Yip, Phys. Rev. B **86**, 064506 (2012).

[14]Recently, V. Vakaryuk [Phys. Rev. B 84, 214524 (2011)] has claimed that by considering the magnetic energy, a mesoscopic sample of Sr$_2$RuO$_4$ could also favor a time-reversal symmetry state. His mechanism, however, is completely different from us.

[15]Equation (2) can also be rewritten as $\{K'_1|\partial_x \eta_x|^2 + K'_2|\partial_y \eta_x|^2 + K'_3(\partial_x \eta_y)(\partial_y \eta_x)^* + K'_4(\partial_y \eta_x)(\partial_x \eta_y)^*\} + \{x \leftrightarrow y\}$, the same form as in Ref. 16 with $K'_1 = K_{1234}$, $K'_2 = K_1$, $K'_3 = K_2$, and $K'_4 = K_3$.

[16]D. F. Agterberg, Phys. Rev. Lett. **80**, 5184 (1998).

[17]V. Ambegaokar, P. de Gennes, and D. Rainer, Phys. Rev. A **9**, 2676 (1974); **12**, 345(E) (1975).

[18]On the other hand, if the higher order terms in Eq. (1) favor a time-reversal symmetric state for the bulk, then the system at $\rho = 1$ would then be either in the A_1 or A_2 phase, thus spontaneously breaking the C_4 rotational symmetry. We thus believe that the speculation in our footnote 27 in Ref. 13 is probably incorrect.

[19]In our previous study[13] in circular disks, we found instead that the critical temperature is independent of the radius R. We speculate that the present suppression of T_c is due to the existence of corners.

[20]G. Sarma, J. Phys. Chem. Solids **24**, 1029 (1963).

[21]We note that our A_1 phase has an order parameter dependent on x but not y. Since the surfaces at $y = 0$ and W are taken to be perfectly reflecting, formally our solution is the same as an infinitely long strip along the y direction, with the order parameter vector forced to be along the x axis. In this case, similar arguments as in Ref. 22 show that, for this infinitely long strip, the system may prefer an Fulde-Ferrell-Larkin-Ovchinnikov-like structure along the y direction, with the relevant wave vector of the order of L^{-1}. Our system instead has finite extent W along the y direction. It remains to be investigated whether an analogous phase can occur in our system, although we suspect that this is somewhat unlikely if W is much less than L.

[22]A. B. Vorontsov, Phys. Rev. Lett. **102**, 177001 (2009).